Arch. Mech., **52**, 4–5, pp. 779–798, Warszawa, 2000

On inelastic impact and dynamic hardness

Dedicated to Professor Zenon Mróz
on the occasion of his 70^{th} birthday

B. STORÅKERS and J. LARSSON

Department of Solid Mechanics
Royal Institute of Technology
S-100 44 Stockholm, Sweden

COLINEAR IMPACT AND DYNAMIC HARDNESS is analysed at spherical contact and moderate strains. A consistent three-dimensional contact theory based on viscoplastic material behaviour is laid down involving elements of self-similarity, stationary boundary conditions and cumulative superposition. Universal relations between impact velocity and the resulting contact region, impression depth and duration of impact are derived. Deformed surface shapes are shown to be self-similar for power law material behaviour and their relation to piling-up and sinking-in is explained in detail. The coefficient of restitution at rebound is estimated to first order. The concept of dynamic hardness is not unequivocally defined in general and various definitions in the literature are discussed in relation to true material rate sensitivity. Theoretical and numerical predictions of the present model are compared with pertinent experimental findings for different metals. Particular features such as lip formation, plastic zone size and maximum penetration depth are elucidated.

1. Introduction

TESTING AT HIGH STRAIN RATES has been of considerable and long standing as related to the constitutive behaviour of materials. Since there is a natural limitation in the traditional uniaxial tensile test at rapid straining, several instrumented tests of different degrees of sophistication have been developed, a prominent one being the split Hopkinson pressure bar, (cf. e.g. TIRUPATAIAH and SUNDARARJAN [30]). More conventional testing is usually carried out by forcing a hard body to strike a deformable solid by fall of gravity, a pendulum machine or a gas gun. In particular, the dynamic hardness of metals and alloys at rapid straining has been tested in this more simple way by many investigators, some also with the purpose to quantify the strain-rate sensitivity of plastic material behaviour as this constituent is needed in many applications. The conversion from measurements of an average hardness value to a constitutive equation where a general relation between stress, strain and strain-rate is to be specified is, how-

ever, not a straightforward matter. Instead, the deformation state at impact by a striking spherical ball is inherently inhomogeneous, and an a priori knowledge of material parameters is, in essence, necessary to interpret the test results properly. It is the present purpose to solve the field equations accurately at spherical impact by means of a prototype viscoplastic constitutive equation and draw pertinent conclusions from earlier experimental findings.

To add some perspective and background to the indentation theory, some momentous achievements will first be sketched briefly. BRINELL [5] invented his test by pressing a hardened ball of a given diameter and load into a solid specimen. The residual area of the imprint was then measured in order to determine the mean pressure or hardness number. MEYER [17] found empirically that for a variety of materials, a power law relation exists between the contact pressure and the radius of the spherical imprint. An extensive experimental investigation was subsequently carried out by NORBURY and SAMUEL [20] who, in particular, examined the form of the Brinell impression in the vicinity of the contact region and whether the material would be raised, piling-up, or the converse, sinking-in. Surface profiles after indentation proved to be self-similar and related to the Meyer formula for several annealed and cold-hammered metals. O'NEILL [22] showed that the Meyer exponent could be directly related to the strain-hardening properties determined by simple tensile testing. TABOR [29] made complete a fully quantitative hardness theory by means of an exhaustive output of experimental data. Two universal parameters were incorporated in the Meyer formula and a measure of representative strain was established.

The approach so far was essentially pragmatic though characterized by a thorough insight. A nonempirical theory, starting from first mechanical principles was proposed by BISHOP, HILL and MOTT [2] who assumed similarity of mode shapes at deep indentation with that of a cavity expanded by internal pressure. This point of view was further elaborated upon e.g. by MARSH [15] and JOHNSON [12]. Solutions of higher accuracy became available with the progress of finite element analysis. Perhaps the first attempt was made by AKYUS and MERWIN [1] analysing circular elastic-plastic indentation in plane strain and numerous analyses were then to follow. An analytical and computational investigation was conducted by HILL, STORÅKERS and ZDUNEK [9] of Brinell indentation of power law hardening solids. Many of the issues posed by Meyer, Norbury and Samuel, O'Neill and Tabor were then given a rigorous theoretical background. In this spirit, analyses based also on flow theory were subsequently made by STORÅKERS and LARSSON [24] for creep, BIWA and STORÅKERS [3] for strain-hardening plasticity and STORÅKERS, BIWA and LARSSON [25] for viscoplasticity.

In a section of his classical monograph, TABOR [29] discussed the case of dynamic hardness combined with experiments performed by impact of spheres mainly under the fall of gravity. Effects of a viscous nature were mentioned but

no influence of true strain-rate sensitivity was detailed. The dynamic analysis was carried out in a quasistatic manner with energy absorbed in wave motion being neglected. A measure of dynamic hardness was determined in an average sense as the quotient between the impact energy and the residual volume made by the imprint. At rebound, a coefficient of restitution was established based on Hertz theory of elastic recovery. Phenomenological though significant results were obtained for the indentation depth and duration of impact as functions of projectile velocity. Further progress was summarized by JOHNSON [13] who besides treating dynamic hardness, discussed also the concept of rebound. For one thing it was made perfectly clear that the coefficient of restitution does not only include material parameters but also depends on the indenter shape and size together with the mass and velocity of the impact.

Numerous experimental investigations have been described in the literature where dynamic hardness has been recorded as a function of impact velocity for different materials and indenter shapes, (cf. e.g. SUBHASH, KOEPPEL and CHANDRA [27]), where in particular, the impact of Vicker's pyramids is treated. In these mainly empirically based investigations, the dynamic hardness is usually compared with its static counterpart and the results depending on the indentation depth and its rate. Any attempt to relate hardness measures to the material flow stress and strain-rate dependence in this way is doomed to be empirical as a material particle in the indented solid experiences a complex history of strain and strain-rate. The celebrated constraint factor, relating hardness to flow stress, by TABOR [29] was, however, given a theoretical background by an axisymmetric solution for spherical indentation of power law hardening materials by HILL *et al.* [9], but a corresponding study for strain-rate sensitive materials is lacking and it is the present objective to provide a remedy. First a rigorous analysis is carried out of single impact of solids which exhibit strain-hardening and true strain-rate sensitivity. The theory is based on a contact analysis by STORÅKERS *et al.* [25] where the power law material behaviour was adopted a priori. The consistent impact results per se will be of interest in different applications such as ballistic penetration and particle erosion, HUTCHINGS [10]. The relation between hardness and flow stress is then discussed in some detail and conclusions are drawn regarding the constitutive behaviour due to hardening and strain-rate effects being of interest at e.g. metal forming analyses and car crash simulations. The theoretical results obtained are compared with pertinent experimental findings, but only a few investigators report also field measurements of inelastic deformation under impact load. TIRUPATAIAH and SUNDARARJAN [30] and OKA, MATSUMURA and FUNAKI [21] stand out in this respect.

2. Elements of the theory of viscoplastic contact

In an attractive monograph by MRÓZ [18], a framework was laid down or the constitutive behaviour of viscous, hardening materials. Two viscous potentials ψ, ϕ were introduced generating stresses, σ_{ij}, and strain rates, $\dot{\varepsilon}_{ij}$, as

$$\sigma_{ij} = \frac{\partial \psi}{\partial \dot{\varepsilon}_{ij}}, \qquad \dot{\varepsilon}_{ij} = \frac{\partial \phi}{\partial \sigma_{ij}} \tag{2.1}$$

related through a Legendre transformation, where

$$D = \sigma_{ij}\dot{\varepsilon}_{ij} = \psi + \phi \tag{2.2}$$

is a dissipation function. In particular, if $\psi(\dot{\varepsilon}_{ij})$ is a homogeneous funcion of degree $(N+1)/N$, then $\phi(\sigma_{ij})$ is by necessity homogeneous of degree $N+1$ due to the duality nature.

A popular and fairly general form of uniaxial material response adoped by MRÓZ [18] reads

$$\sigma = \sigma_0 \varepsilon^M \left(\frac{\dot{\varepsilon}}{\dot{\varepsilon}_0}\right)^N, \tag{2.3}$$

where M, N are positive exponents and σ_0 is a constitutive parameter, $\dot{\varepsilon}_0$ leing a reference strain-rate. Although specialized, Eq. (2.3) may represent a wide range of material behaviour. In its complete form it reproduces primary creep, NADAI [19], or strain-rate sensitive plasticity, GHOSH [7]. In degenerated forms when $M = 0$, Eq. (2.3) reduces to Norton's law for stationary creep and when $N = 0$, to strain-hardening plasticity. Equations (2.1) to (2.3) were adopted in a multiaxial form based on von Mises flow by STORÅKERS *et al.* [25] in order to analyse indentation of viscoplastic solids. A general theory was laid down for a family of indenters, their shapes being characterized by smooth homogeneous functions. Here a brief account will be given and confined to axisymmetric indenters having a spherical shape.

In Fig. 1a, a rigid indenter having a spherical, or locally parabolic, shape within Hertzian kinematics is depicted. When formulating an associated boundary value problem, the only nonhomogeneous boundary condition reduces to

$$u_3 = h - r^2/D, \qquad x_3 = 0, \quad r \leq a. \tag{2.4}$$

With the present constitutive equation in mind, a rate formulation isnecessary and accordingly by Eq. (2.4)

$$\dot{u}_3 = \dot{h}, \qquad x_3 = 0, \quad r \leq a, \tag{2.5}$$

where a dot denotes differentiation with respect to natural time.

Reduced variables were introduced a priori by

$$x_i = a\tilde{x}_i, \qquad \dot{u}_i = \dot{h}\tilde{u}_i(\tilde{x}_k) \tag{2.6}$$

which has far-reaching consequences as the boundary condition, Eq. (2.5), reduces to

$$\tilde{u}_3 = 1, \qquad \tilde{x}_3 = 0, \quad \tilde{r} \leq 1. \tag{2.7}$$

As seen in Fig. 1, the original problem having a moving boundary and thus incomplete contact is now transformed to an intermediate problem constituting indentation of a circular flat punch (Boussinesq's problem), being well suited for numerical analysis based on finite elements. The solution to the original problem based on a spherical shape may then be accomplished by simple cumulative superposition.

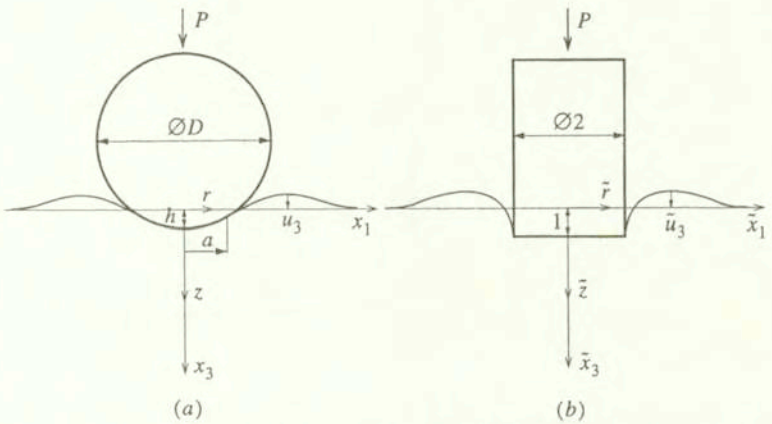

FIG. 1. a) The original contact problem (Brinell); b) The reduced, intermediate problem (Boussinesq).

HILL *et al.* [9] proved that for deformation theory of plasticity, spherical indentation possesses self-similarity for power law hardening materials. In particular it was shown that the expression

$$c_2 = \frac{a^2}{hD} \tag{2.8}$$

is an invariant where c_2 depends solely on the hardening exponent solely. In passing it may be noted that a similar relation for c_p holds true for any homogeneous shape p, STORÅKERS *et al.* [24], where for instance $p = 1$ corresponds to a cone or a pyramid.

The use of an intermediate flat die field to solve problems for a curved indenter was analysed in detail by SPENCE [23] for linear elastic materials. This procedure

was subsequently proved to hold true for normal indentation of nonlinear solids by STORÅKERS *et al.* [3, 24, 25] and more recently by LARSSON and STORÅKERS [14] for oblique indentation.

It may first be observed by introducing Eq. (2.8) into (2.4) that

$$u_3 = h(1 - c_2 r^2/a^2) \tag{2.9}$$

which physically implies that at the contact contour, either the material piles up or sinks in whether c_2 exceeds unity or not.

STORÅKERS *et al.* [25] carried out full finite element solutions to viscoplastic solids for the frictionless flat die problem and subsequently obtained results for spherical dies according to Fig. 2. Ordinarily the invariant c_2 is a general function of the material exponents but as may be seen in Fig. 2, $c_2 = c_2(M + N)$ holds within a very high accuracy. For this finding to be exact, partial proportional straining is required.

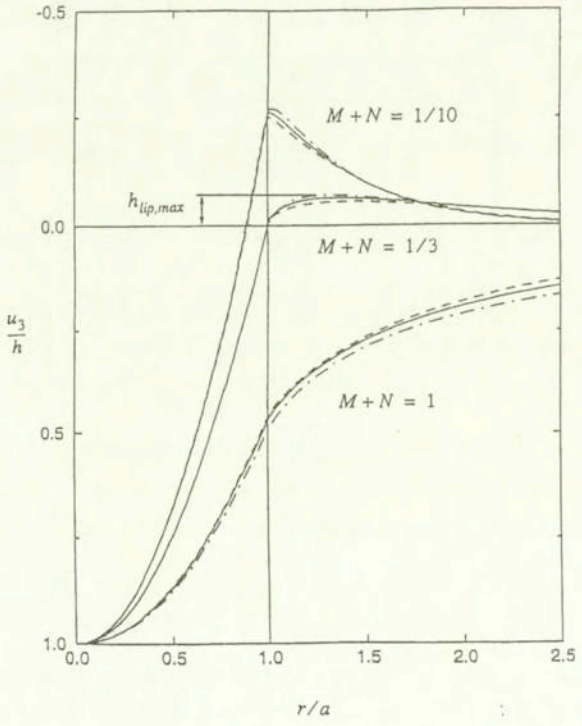

FIG. 2. Deformed surface shapes at spherical indentation of viscoplastic materials for $M + N = 1, 1/3, 1/10$; (—) general viscoplasticity ($M = N$) STORÅKERS, BIWA and LARSSON [25], (- - -) plastic flow theory ($N \to 0$) BIWA and STORÅKERS [3] (– · – · –) creep theory ($M \to 0$) STORÅKERS and LARSSON [24].

For a representative set of M, N values it was found that

$$c_2 = 1.45e^{-(M+N)} \tag{2.10}$$

constitutes a very good approximation for $0 \leq M + N \leq 1$.

Again referring to the notation in Fig. 1a it may readily be shown that the mean pressure at contact may be expressed in the form

$$\frac{P}{\pi a^2} = \sigma_0 \alpha(M,N) \left[\beta_M(M,N)\frac{a}{D}\right]^M \left[\beta_N(M,N)\frac{\dot{a}}{\dot{\varepsilon}_0 D}\right]^N, \tag{2.11}$$

where α, β_M and β_N are universal parameters to be determined. It may be noted that TABOR [29] in his classical empirical investigations of plastic strain-hardening materials correspondingly found $\alpha = 2.8$, $\beta_M = 0.4$.

From a numerical solution of representative M, N values, STORÅKERS *et al.* [25] found for viscoplastic solids that Eq. (2.11) is well reproduced by

$$\frac{P}{\pi a^2} = 3(1+2N)\sigma_0 \left(\frac{a}{3D}\right)^M \left(\frac{\dot{a}}{3\dot{\varepsilon}_0 D}\right)^N. \tag{2.12}$$

So far, the results of the analysis have been given only for a rigid spherical indenter pressed into a viscoplastic half-space. Should normal contact occur between two deforming spheres of different diameters and strength but having the same material exponents, the original results may readily be generalized by replacing the single material constant σ_0 by σ_1 and σ_2, respectively, and the diameter D by D_1 and D_2. Accordingly, STORÅKERS *et al.* [25] showed that by introducing

$$\frac{1}{\sigma_0^{1/q}} = \frac{1}{\sigma_1^{1/q}} + \frac{1}{\sigma_2^{1/q}} \tag{2.13}$$

where $q = M + N$ and

$$\frac{1}{D} = \frac{1}{D_1} + \frac{1}{D_2}, \tag{2.14}$$

then the solution for the half-space problem immediately generates a solution for the two-body problem. The matter was further discussed in more detail by STORÅKERS [26].

3. Analysis of colinear impact

For a start, the equation of motion for the mass centres of two colinearly colliding bodies yields

$$P = -m_1\dot{v}_1 = m_2\dot{v}_2 \tag{3.1}$$

with notation according to Fig. 3 and again, a dot denotes differentiation with respect to natural time.

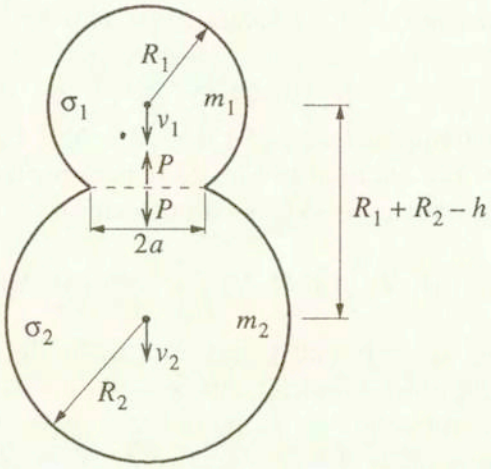

FIG. 3. Colinear collision of two dissimilar spheres.

The local velocities are then related to the approach, h, by

$$\nu_1 - \nu_2 = \dot{h}. \tag{3.2}$$

Introducing a combined mass by

$$\frac{1}{m} = \frac{1}{m_1} + \frac{1}{m_2} \tag{3.3}$$

and using Eqs. (3.1) and (3.2) yields

$$P = -m\ddot{h}. \tag{3.4}$$

At moderate velocities, when the propagation of waves may be neglected, the global constitutive Eq. (2.12) may be adopted in the form

$$P = \gamma\sigma_0 D^2 \left(\frac{h}{D}\right)^{1+(M-N)/2} \left(\frac{\dot{h}}{\dot{\varepsilon}_0 D}\right)^N, \tag{3.5}$$

where σ_0 and D are given by Eqs. (2.13) and (2.14) respectively, and where, on introducing Eq. (2.8),

$$\gamma = 3^{1-M-N} 2^{-N} (1 + 2N)\pi c_2^{1+(M+N)/2}. \tag{3.6}$$

Combining Eqs. (3.4) and (3.5) then yields

$$\ddot{h} + \frac{\gamma}{m}\sigma_0 D^2 \left(\frac{h}{D}\right)^{1+(M-N)/2} \left(\frac{\dot{h}}{\dot{\varepsilon}_0 D}\right)^N = 0. \tag{3.7}$$

The first integral of Eq. (3.7) gives

$$\dot{h}^{2-N} + \frac{2(2-N)\gamma\sigma_0 D^{1-(M+N)/2}}{(4+M-N)\dot{\varepsilon}_0^N m} h^{2+(M-N)/2} = C, \tag{3.8}$$

where C is a constant.

From the initial conditions $h(0) = 0$, $\dot{h}(0) = \nu_1(0) - \nu_2(0) = \nu_0$, the constant C in Eq. (3.8) becomes

$$C = \nu_0^{2-N}. \tag{3.9}$$

By Eqs. (3.8) and (3.9), the maximum approach depth, h_m, say, at rebound, $\dot{h} = 0$, follows as

$$h_m = D\left[\frac{\left(1+\frac{M+N}{2(2-N)}\right)\dot{\varepsilon}_0^2 m}{\gamma\sigma_0 D}\right]^{\frac{2}{4+M-N}} \left(\frac{\nu_0}{\dot{\varepsilon}_0 D}\right)^{\frac{2(2-N)}{4+M-N}} \tag{3.10}$$

and accordingly, the approach rate

$$\dot{h} = \dot{\varepsilon}_0 D\left[\frac{\gamma\sigma_0 D}{\left(1+\frac{M+N}{2(2-N)}\right)\dot{\varepsilon}_0^2 m}\left(\frac{h_m}{D}\right)^{2+(M-N)/2}\left(1-\left(\frac{h}{h_m}\right)^{2+(M-N)/2}\right)\right]^{\frac{1}{2-N}}. \tag{3.11}$$

By Eqs. (2.8), (3.5) and (3.11), the hardness value becomes

$$\frac{P}{\pi a^2} = \frac{\gamma\sigma_0}{\pi c_2}\left[\frac{\gamma\sigma_0 D}{\left(1+\frac{M+N}{2(2-N)}\right)\dot{\varepsilon}_0^2 m}\right]^{\frac{N}{2-N}} \left(\frac{h_m}{D}\right)^{\frac{M+N}{2-N}} \left(\frac{h}{h_m}\right)^{\frac{M-N}{2}}\left[1-\left(\frac{h}{h_m}\right)^{2+(M-N)/2}\right]^{\frac{N}{2-N}}. \tag{3.12}$$

The impact time as a function of indentation depth is given by simple quadrature of Eqs. (3.8) to (3.10) as

$$t = \dot{\varepsilon}_0^{-1}\left[\frac{\left(1+\frac{M+N}{2(2-N)}\right)\dot{\varepsilon}_0^2 m}{\gamma\sigma_0 D}\right]^{\frac{1}{2-N}} \left(\frac{D}{h_m}\right)^{\frac{M+N}{2(2-N)}} \int_0^{h/h_m} \frac{dx}{\left(1-x^{2+(M-N)/2}\right)^{1/(2-N)}}, \tag{3.13}$$

or by Eq. (3.10)

$$t = \frac{h_m}{\nu_0} \int_0^{h/h_m} \frac{dx}{\left(1 - x^{(4+M-N)/2}\right)^{1/(2-N)}}. \tag{3.14}$$

The impact time, t_m, at maximum approach, $h = h_m$, may be expressed by means of the gamma function, Γ, used in Euler's integral in Eq. (3.14), as

$$t_m = \frac{h_m}{\nu_0} \frac{2}{4+M-N} \frac{\Gamma\left(\dfrac{2}{4+M-N}\right)\Gamma\left(\dfrac{1-N}{2-N}\right)}{\Gamma\left(1 - \dfrac{M+N}{(2-N)(4+M-N)}\right)}, \tag{3.15}$$

(cf. also BORODICH [4]).

The approach time is only weakly dependent on the impact velocity. In particular at perfectly plastic contact, $M = N = 0$, the time as a function of the approach, Eq. (3.13), reduces to

$$t = \frac{2}{\pi} t_m \arcsin\left(\frac{\pi h}{2 t_m \nu_0}\right), \tag{3.16}$$

where

$$t_m = \left(\frac{\pi m}{12 c_2 \sigma_0 D}\right)^{1/2} \tag{3.17}$$

from Eqs. (3.6), (3.10) and (3.15) and accordingly, independent of the initial velocity.

TABOR [29] proposed a frequently used and simple dynamic hardness number, $H_{DT} = W/V$, in an average sense where

$$W = \frac{m\nu_0^2}{2} \tag{3.18}$$

is the energy at initial impact, and

$$V = \pi \int_0^{h_m} a^2 dh \tag{3.19}$$

is the residual imprint volume, (cf. Fig. 1a).

Based on the present theory, Tabor's hardness number may be readily determined by Eqs. (2.8), (3.10), (3.18) and (3.19) to yield

$$H_{DT} = \frac{\gamma\sigma_0}{\pi c_2 \left(1 + \dfrac{M+N}{2(2-N)}\right)} \left[\frac{\gamma\sigma_0 D}{\left(1 + \dfrac{M+N}{2(2-N)}\right)\dot{\varepsilon}_0^2 m}\right]^{\frac{N}{2-N}} \left(\frac{h_m}{D}\right)^{\frac{M+N}{2-N}}. \tag{3.20}$$

When analysing the forward contact collision at fully inelastic behaviour, the influence of elasticity was neglected. At rebound, however, purely elastic response is to be expected and will possibly prevail for the remaining duration of contact. This is not a quite straight-forward matter to analyse but a simple estimate could be made to first order.

It may first be observed that with the constitutive equation presently adopted, the load at maximum approach will vanish, Eq. (3.12), and accordingly, the rebound velocity will reduce to nil. At purely plastic impact, however, the contact force, Eq. (3.12), will attain its maximum value at the rebound event and with the pressure and conjugate elastic surface displacement distributions available, determination of the coefficient of restitution could be made to first order.

The coefficient of restitution, e, is defined as

$$e^2 = \frac{W_e}{W} \tag{3.21}$$

where again W is the impact energy at initial contact and W_e is the released energy at rebound or equivalently

$$e = \frac{\nu_e}{\nu_0}, \tag{3.22}$$

where ν_e is the velocity when the colliding particles separate.

The energy dissipated at forward motion may immediately be determined by means of Eqs. (3.18) and (3.20) to read

$$W = \frac{\gamma \sigma_0 D^3}{2 + M/2} \left(\frac{h_m}{D} \right)^{2+M/2} \tag{3.23}$$

at nonviscous contact, $N = 0$.

As to the determination of the released energy, in Fig. 4 the pressure distributions determined from flow theory by BIWA and STORÅKERS [3] are depicted for a range of values of the strain-hardening exponent M. As may be seen, they deviate considerably from the Hertzian elliptical distribution. In case of perfect plasticity, $M = 0$, the contact pressure, p_m, is approximately uniform and an analytical estimate may then be carried out.

The conjugate elastic surface displacement distribution is well known, (cf. e.g. JOHNSON [13], p. 57), and reads

$$u_z = \frac{4 p_m a}{\pi \overline{E}} E(r/a), \tag{3.24}$$

where $1/\overline{E} = (1 - \nu_1^2)/E_1 + (1 - \nu_2^2)/E_2$ and $E(r/a)$ is the complete elliptical integral of the second kind with modulus r/a. $E(0) = \pi/2$.

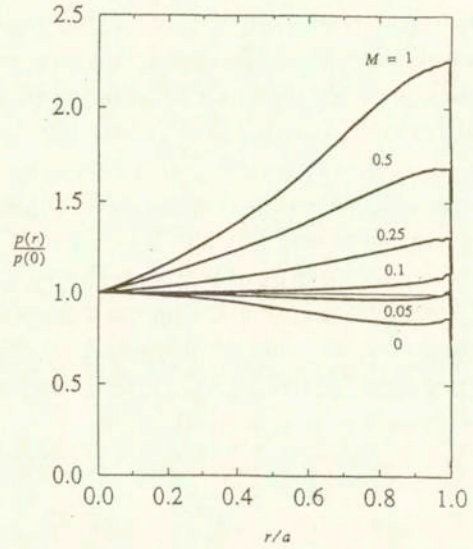

FIG. 4. Normalized contact pressure distribution when $M = 1, 0.5, 0.25, 0.1, 0.05$ and 0 for spherical contact by flow theory.

The energy loss at rebound is then simply $\pi p_m \overline{u} a^2/2$ where $\overline{u}$ is the mean displacement or explicitly

$$\overline{u} = \frac{16 p_m a}{3\pi \overline{E}}, \tag{3.25}$$

and accordingly

$$W_e = \frac{8 p_m^2 a^3}{3\overline{E}}. \tag{3.26}$$

At perfect plasticity, from the above results it may be concluded that $p_m = 3\sigma_0$, Eq. (2.12), and $a^2 = 3Rh_m$, Eqs. (2.8) and (2.10), approximately. The elastic energy loss then reduces to

$$W_e = \frac{72\sqrt{3}\sigma_0^2 (Rh_m)^{3/2}}{\overline{E}} \tag{3.27}$$

and the impact energy, Eq. (3.23), to

$$W = \frac{9}{2}\pi \sigma_0 R h_m^2 \tag{3.28}$$

if c_2 is set to 3/2.

Thus the coefficient of restitution becomes

$$e^2 = \frac{16\sqrt{3}\sigma_0}{\pi \overline{E}} \left(\frac{R}{h_m}\right)^{1/2}. \tag{3.29}$$

Since from Eq. (3.10)

$$h_m = \left(\frac{m}{9\pi\sigma_0 R}\right)^{1/2} \nu_0, \tag{3.30}$$

then by Eq. (3.30)

$$e^2 = \frac{16\sqrt{3}\sigma_0}{\pi \overline{E}} \left(\frac{9\pi\sigma_0 R^3}{m\nu_0^2}\right)^{1/4}. \tag{3.31}$$

As it has been pointed out earlier by JOHNSON [13], the restitution coefficient is not a single material parameter but depends on the geometry of contact and the mass and velocity of initial impact.

A relation similar to Eq. (3.31) was proposed by JOHNSON [13] and the difference, of the order of 20%, reduces only to a constant. This is due to the present account of piling-up and to the fact that the true pressure distribution, in contrast to the Hertzian one, was used at energy release. Some supporting experimental results by GOLDSMITH [8] are seen to be of the relation $e \sim \nu_0^{-1/4}$, Eq. (3.31), as reproduced in Johnson's monograph [13].

4. Experimental aspects and discussion

Some major assumptions and approximations introduced above in the impact analysis will be briefly discussed. The dynamic analysis was carried out with influence of wave motion neglected. This is relevant if the impact velocity is much smaller compared with the elastic wave speed. In the present context and ordinary circumstances in general, it has been estimated by JOHNSON [13] that for shallow imprints, the assumption is tolerable if the impact velocity is less than 500 m/s, approximately. More precisely, TIRUPATAIAH and SUNDARARJAN [30] found in their dynamic tests of copper and iron at recorded impact velocities of 180 m/s by WC balls of 4.67 mm diameter, that the energy loss due to stress waves was within a few per cent. Likewise TIRUPATAIAH and SUNDARARJAN [30] found that the difference between adiabatic and isothermal flow properties was of the same order.

A measure, Λ, in order to quantitatively categorize different regimes of elasto-plastic indentation was proposed by JOHNSON [12] as

$$\Lambda = \frac{Ea}{(1-\nu^2)\sigma_y R} \tag{4.1}$$

in the present notation, where σ_y is the flow stress at a representative strain magnitude

$$\varepsilon = 0.2a/R \tag{4.2}$$

as established by TABOR [29].

From an elastic-plastic finite element analysis, BIWA and STORÅKERS [3] found for a variety of representative materials, that for $\Lambda > 30$ fully plastic flow was reasonably well attained at $a/R > 0.03$. At continued indentation and increasing contact, the accuracy of the present theory based on linear kinematics deteriorates at large strains and the assumptions are less well fulfilled when a/R becomes a decade higher, (cf. MESAROVIC and FLECK [16]). The impact analysis was further carried out at vanishing frictional contact. It is well known, however, that for lumped relations such as between loading, indentation depth and contact region, frictional effects will only slightly affect the results, CARLSSON, LARSSON and BIWA [6].

As a principal finding above, the dynamic hardness value $H_D = P/\pi a^2$ was derived as a function of the indentation depth, h, by Eq. (3.12). It is clear that any effort to derive uniquely a material constraint factor to convert the experimentally determined dynamic hardness values to their static counterparts will not be successful. The mass and the radius of an impacting sphere will be essential parameters as was also the case for the coefficient of restitution, Eq. (3.30) above. A still more striking obstacle remains to relate the dynamic hardness to material flow stress-strain data. It may also be noted from Eq. (3.12) that the influence of piling-up behaviour, as governed by the invariant c_2 in Eq. (2.8), has only a weak influence of hardness when remembering the factor γ from Eq. (3.6).

Before trying to correlate the theoretical findings with experimental results, it should be stressed that by the adopted constitutive Eq. (2.3), both at initial impact and at rebound, the hardness measure vanishes when both the strain-hardening and rate sensitivity are taken into account. Remembering though that this simple prototype model comprises only three parameters to vary and to simulate a wide spectrum including especially low strain-rates, obviously the constitutive equation should include a cut-off stress.

At any instant during the impact process, h/h_m, it may be seen from Eq. (3.13), however, that the dynamic hardness is related to the absolute indentation depth, h, as

$$H_D \sim h^{\frac{M+N}{2-N}}. \tag{4.3}$$

The same dependence also follows if the present analysis is applied to Tabor's estimate, Eq. (3.20).

Using Tabor's measure of representative strain, Eq. (4.2), and the invariant, Eq. (2.8), an apparent measure of dynamic hardness can now be determined by means of Eq. (4.3)

$$H_D \sim \varepsilon^{M+N} \tag{4.4}$$

to the first order as N is ordinarily of the order of 0.1.

An extensive number of experimental investigations of inelastic impact with associated determination of hardness has been presented over the years, for a recent account cf. e.g. TIRUPATAIAH and SUNDARARJAN [31]. However, residual deformation fields are seldom measured and recorded and for this reason only the results of two investigations are examined in some detail. First an admirably careful and thorough investigation was carried out by TIRUPATAIAH and SUNDARARJAN [30] who, by the impact of spherical WC balls of diameter 4.67 mm, determined the dynamic properties of annealed copper and iron over a considerable range of impact velocities of up to 200 m/s. This was achieved by means of a gas gun for high velocities while a gravity drop tower was used for lower velocities, 10 m/s, for accuracy. Dynamic hardness was determined using Tabor's method with elastic effects neglected. Also residual surface profiles outside the contact region, lip formation, were recorded using a digital height measuring equipment with a resolution of 1 μm.

TIRUPATAIAH and SUNDARARJAN [30] observed that the hardness values showed both strain-hardening and rate-sensitivity effects. They found that the dynamic hardness was in excess of 30% compared to static values for copper in the particular circumstances prevailing. At ordinary Brinell testing the hardening exponents, M, were found for copper and iron resulting in 0.41 and 0.31, respectively. At high strain rates, up to 10^4 s^{-1}, the corresponding exponents, $M + N$, for apparent strain-hardening, Eq. (4.4), were 0.56 and 0.18 respectively. It is interesting to notice then, as was also concluded by TIRUPATAIAH and SUNDARARJAN [30], that the tests on iron exhibited strain-rate softening and accordingly, a negative value of the strain-rate exponent, N. As has already been stated, the simple form of the constitutive Eq. (2.3) may not be used for consistency for any strain-rates. In a restricted region, the theoretical predictions of Fig. 2 as regards piling-up or sinking-in and based on the exponents M, N, may be put to trial when comparing experimental recordings of lip formation. More recently, SUNDARARJAN and TIRUPATAIAH [28] determined the exponents for several more metals and alloys by impact experiments. In the data, both significant strain-rate hardening and softening, respectively, were found. However, no corresponding field measurements of deformation profiles were recorded.

In Fig. 5, the experimentally determined residual surface profiles are reproduced from the tests by TIRUPATAIAH and SUNDARARJAN [30] at representative strains of about 7%. It may first be seen that the surface heights of the two materials investigated are of different orders of magnitude and it is difficult to observe any difference between the dynamic and static results. For copper ($M = 0.41, N = 0.15$) as depicted in Fig. 5a, the developed lip profile is not very pronounced but a very modest sinking-in behaviour is perceptible. This is in accordance with the predictions shown in Fig. 2 as the relative profiles depend only on $M + N$ and when the combined exponent is 0.56, a slight sinking-in will

result. More precisely for $M = 0.5$ it was shown by BIWA and STORÅKERS ([3], Fig. 3) that the maximum lip height occurs at $r/a = 2$. In Fig. 5b where results from iron, $M + N = 0.18$, are shown, the lip profiles clearly exhibit piling-up behaviour again in agreement with Fig. 2.

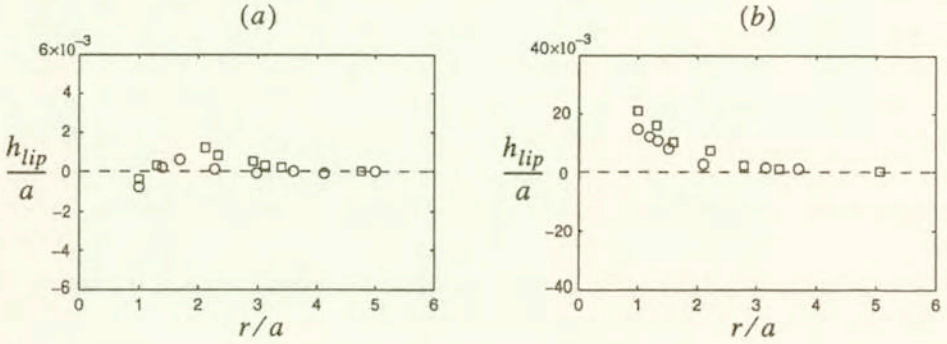

FIG. 5. Dimensionless surface profiles at dynamic impact (□) and static indentation (○); a) Copper; dynamic: $\varepsilon = 7.92\%$ and static: $\varepsilon = 7.79\%$; b) Iron; dynamic: $\varepsilon = 6.88\%$ and static $\varepsilon = 6.3\%$. Experimental data according to TIRUPATAIAH and SUNDARARAJAN [30].

TIRUPATAIAH and SUNDARARJAN [30] concluded from their experimental findings that in the case of copper, static and dynamic profiles coincided which is obvious from the background just given. For iron, however, at straining of 8%, a distinction was observed as shown in Fig. 6 where the maximum lip height is recorded as a function of representative strain by TIRUPATAIAH and SUNDARARJAN [30]. Thus strain-rate softening behaviour, $N < 0$, causes an increase in lip height as is evident in Fig. 2.

OKA, MATSUMURA and FUNAKI [21] investigated dynamic and static indentation of hard steel balls on substrates made of annealed commercially pure aluminium, iron and gray cast iron. Lip heights were recorded by a surface profilometer and strain distributions were measured by a photoengraving method. Most of the experimental observations were made at impact velocities of 200 m/s and the depth of indentations produced was indeed large, $a/R \sim 1$. This is far beyond the assumptions made in the present theory. For moderate imprints, however, dimensionless lip heights are shown in Fig. 7 reproduced from tests on aluminium and iron conducted by OKA *et al.* [21]. No quantitative conclusions may be drawn from the comparison with the present predictions, as no hardening properties were recorded. In Fig. 7a, applicable to aluminium, it may be seen that within the scatter present, the relative lip height is depth-independent, implying self-similar behaviour and that the material is strain-rate hardening. For iron, Fig. 7b, the results are less consistent but there is an indication of strain-rate softening behaviour as was the case also in the investigation made

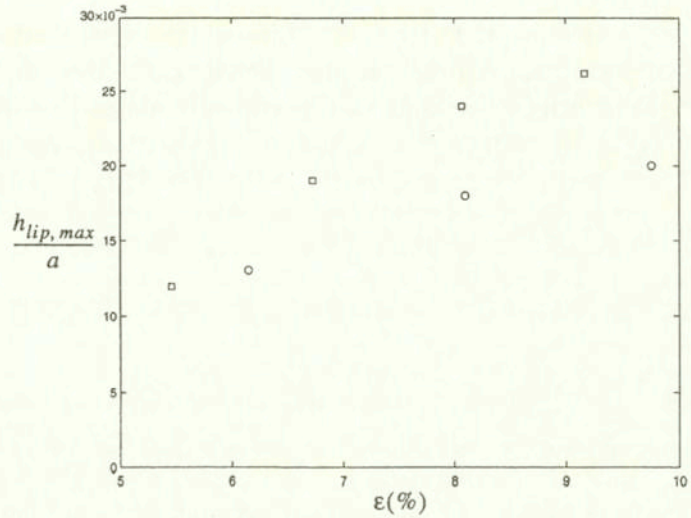

FIG. 6. Dimensionless ratio of maximum lip height to contact radius versus average strain at dynamic impact (□) and static indentation (○). Experimental data for iron according to TIRUPATAIAH and SUNDARARAJAN [30].

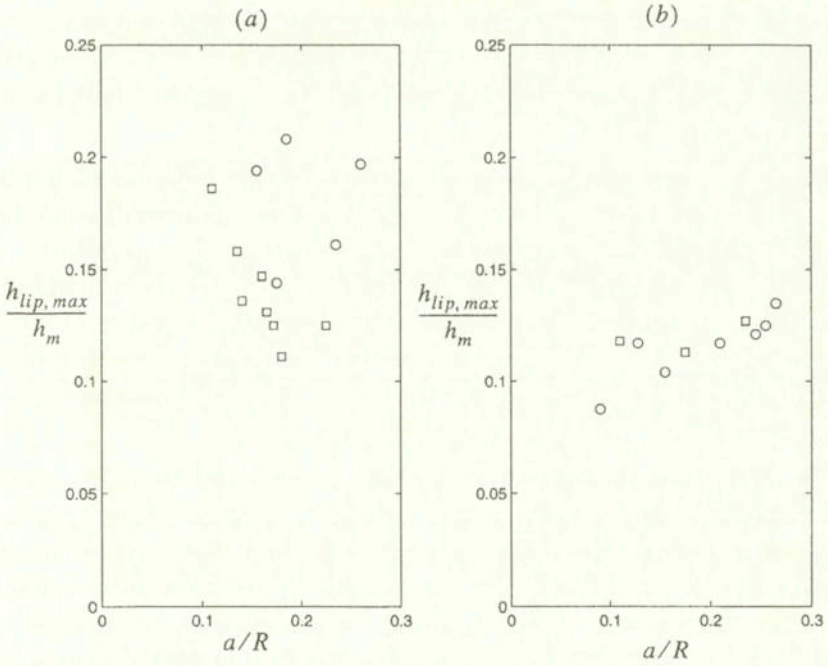

FIG. 7. Dimensionless ratio of maximum lip height to depth of indentation versus average deformation. Experimental data for dynamic impact (□) and static indentation (○) according to OKA *et al.* [21]; (a) Aluminium, (b) Iron.

by TIRUPATAIAH and SUNDARARJAN [30]. In analogy, the relative size of the plastic region increased for aluminium and decreased for iron at high strain-rates. Related phenomena may occur also in other circumstances. For instance, it has been shown by HUTCHINSON and NEALE [11] that for materials whose response is strain-rate sensitive, a considerable delay in necking at uniaxial tension arises.

5. Conclusion

Spherical impact at moderate inelastic strains was studied at quasistatic, frictionless contact by means of a three-dimensional analysis for viscoplastic solids. The constitutive equation was admittedly simple but strain-hardening and strain-rate sensitivity effects were taken into explicit account by power law exponents. A dynamic hardness measure, mean pressure resistance, was derived and it was found that besides the indentation depth, the hardness number necessarily depends on a combination of initial impact velocity, mass and radius of the projectile. Any relation between dynamic hardness and material flow stress must include these variables and also requires a full constitutive equation to be known in advance. Thus essentially, the problem posed has to be solved in an inverse manner and the present theory was intended to fill such a gap in a first tentative way.

At dynamic hardness it was shown that an apparent measure of hardness could be found simply by adding the ordinary power law exponent of static hardening to the presently introduced rate-sensitivity exponent. This proved to be in conformity with experimental findings. A crucial test of the three-dimensional analysis proved to be a correlation with experimental measurements of residual surface profiles. It was found that the presence of the strain-rate sensitivity exponent gave predictions of correct order with the compound hardening exponent introduced.

It is believed that the theoretical results are computationally highly accurate as they are based on self-similarity and a careful finite element procedure. A drawback is that the elastic effects are not taken directly into account and that the viscoplastic material law was based only on one strength parameter and two exponents. With the present purpose in mind, the influence of elasticity is not a primary issue but to improve the model, a greater range of strain-rates is more urgent. This could preferably be done by first introducing a cut-off stress. The price to be paid is that the computational work will be expected to become more cumbersome as self-similarity will be lost.

References

1. F. A. AKYUS and J. E. MERWIN, *Solution of the nonlinear problems of elastoplasticity by finite element methods*, AIAA J., **6**, 1825–1831, 1968.
2. R. F. BISHOP, R. HILL and N. F. MOTT, *The theory of indentation and hardness tests*, Proc. Phys. Soc., **57**, 147–159, 1945.
3. S. BIWA and B. STORÅKERS, *An analysis of fully plastic Brinell indentation*, J. Mech. Phys. Solids, **43**, 1303–1333, 1995.
4. F. M. BORODICH, *The Hertz frictional contact between nonlinear elastic anisotropic bodies (the similarity approach)*, Int. J. Solids Structures, **30**, 1513–1526, 1993.
5. J. A. BRINELL, *Mémoire sur les épreuves à bille en acier*, Congrés International des Méthodes d'Essai des Matériaux de Construction (Paris), tome 2, 83–94, 1901.
6. S. CARLSSON, P.-L. LARSSON and S. BIWA, *On frictional effects at inelastic contact between spherical bodies*, Int. J. Mech. Sci., **42**, 107–128, 2000.
7. A. K. GHOSH, *The influence of strain hardening and strain-rate sensitivity on sheet metal forming*, J. Eng. Mat. Tech., **99**, 264–274, 1977.
8. W. GOLDSMITH, *Impact*, London: Arnold 1960.
9. R. HILL, B. STORÅKERS and A. ZDUNEK, *A theoretical study of the Brinell hardness test*, Proc. R. Soc. Lond., **A423**, 301–330, 1989.
10. I. M HUTCHINGS, *A model for the erosion of metals by spherical particles at normal incidence*, Wear, **70**, 269–281, 1981.
11. J. W. HUTCHINSON and K. W. NEALE, *Influence of strain-rate sensitivity on necking under uniaxial tension*, Acta Metall., **25**, 839–846, 1977.
12. K. L. JOHNSON, *The correlation of indentation experiments*, J. Mech. Phys. Solids, **18**, 115–126, 1970.
13. K. L. JOHNSON, *Contact mechanics*, Cambridge University Press, Cambridge 1985.
14. J. LARSSON and B. STORÅKERS, *Oblique indentation of creeping solids*, Euro. J. Mech. A/Solids, **19**, 565–584, 2000.
15. D. M. MARSH, *Plastic flow in glass*, Proc. Roy. Soc. Lond., **A279**, 420–435, 1964.
16. S. D. MESAROVIC and N. A. FLECK, *Spherical indentation of elastic-plastic solids*, Proc. R. Soc. Lond., **A455**, 2707–2728, 1999.
17. E. MEYER, *Untersuchen über Härtepräfung und Härte*, Z. ver. deutcher Ing., **52**, 645–654, 1908.
18. Z. MRÓZ, *Mathematical models of inelastic material behaviour*, Solid Mechanics Division, University of Waterloo, Waterloo, Ontario 1973.
19. A. NADAI, *The influence of time upon creep: the hyperbolic creep law*, S .Timoshenko Anniversary Volume, McMilan Co, New York 1938.
20. A. L. NORBURY and T. SAMUEL, *The recovery and sinking-in or piling-up of material in the Brinell test, and the effect of these factors on the correlation of the Brinell with certain other hardness tests*, J. Iron Steel Inst., **117**, 673–687, 1928.
21. Y. I. OKA, M. MATSUMURA and H. FUNAKI, *Measurements of plastic strain below an indentation and piling-up between two adjacent indentations*, Wear, **186–187**, 50–55, 1995.
22. H O'NEILL, *The significance of tensile and other mechanical test properties of metals*, Proc. Inst. Mech. Engng., **151**, 116–130, 1944.

23. D. A. SPENCE, *Self similar solutions to adhesive contact problems with incremental loading*, Proc. Roy. Soc. Lond., **A305**, 55–80, 1968.

24. B. STORÅKERS and P.-L. LARSSON, *On Brinell and Boussinesq indentation of creeping solids*, J. Mech. Phys. Solids, **42**, 307–332, 1994.

25. B. STORÅKERS, S. BIWA and P.-L. LARSSON, *Similarity analysis of inelastic contact*, Int. J. Solids Structures, **34**, 3061–3083, 1997.

26. B. STORÅKERS, *Local contact behaviour of viscoplastic particles*, IUTAM Symposium on Mechanics of Granular and Porous Materials, Kluwer Academic Publishers, 173–184, 1997.

27. G. SUBHASH, B. J. KOEPPEL and A. CHANDRA, *Dynamic indentation hardness and rate sensitivity in metals*, J. Eng. Mat. Tech., **121**, 257–263, 1999.

28. G. SUNDARARAJAN and Y. TIRUPATAIAH, *The hardness-flow stress correlation in metallic materials*, Bull. Mat. Sci., **17**, 747–770, 1994.

29. D. TABOR, *Hardness of metals*, Clarendon Press, Oxford 1951.

30. Y. TIRUPATAIAH and G. SUNDARARAJAN, *A dynamic indentation technique for the characterization of the high strain rate plastic flow behaviour of ductile metals and alloys*, J. Mech. Phys. Solids, **39**, 243–271, 1991.

31. Y. TIRUPATAIAH and G. SUNDARARAJAN, *The strain-rate sensitivity of flow stress and strain-hardening rate in metallic materials*, Mat. Sci. Engng., **A189**, 117–127, 1994.

Received March 24, 2000.